REPORT DOCUMENTATION PAGE

Form Approved
OMB No. 0704-0188

PLEASE DO NOT RETURN YOUR FORM TO THE ABOVE ORGANIZATION.

1. REPORT DATE *(DD-MM-YYYY)*	2. REPORT TYPE	3. DATES COVERED *(From - To)*
31-05-2013	Journal Article	

4. TITLE AND SUBTITLE
Optical turbulence on underwater image degradation in natural environments

5a. CONTRACT NUMBER

5b. GRANT NUMBER

5c. PROGRAM ELEMENT NUMBER
0602782N

6. AUTHOR(S)
Weilin Hou, Sarah Woods, Ewa Jarosz, Wesley Goode, and Alan Weidemann

5d. PROJECT NUMBER

5e. TASK NUMBER

5f. WORK UNIT NUMBER
73-6369-01-5

7. PERFORMING ORGANIZATION NAME(S) AND ADDRESS(ES)
Naval Research Laboratory
Oceanography Division
Stennis Space Center, MS 39529-5004

8. PERFORMING ORGANIZATION REPORT NUMBER
NRL/JA/7320-11-843

9. SPONSORING/MONITORING AGENCY NAME(S) AND ADDRESS(ES)
Office of Naval Research
One Liberty Center
875 North Randolph Street, Suite 1425
Arlington, VA 22203-1995

10. SPONSOR/MONITOR'S ACRONYM(S)
ONR

11. SPONSOR/MONITOR'S REPORT NUMBER(S)

12. DISTRIBUTION/AVAILABILITY STATEMENT
Approved for public release, distribution is unlimited.

13. SUPPLEMENTARY NOTES

14. ABSTRACT

It is a well-known fact that the major degradation source on electro-optical imaging underwater is from scattering by particles of various origins and sizes. Recent research indicates that, under certain conditions, the apparent degradation could also be caused by the variations of index of refraction associated with temperature and salinity microstructures in the ocean and lakes. The combined impact has been modeled previously through the simple underwater imaging model. The current study presents the first attempts in quantifying the level of image degradation due to optical turbulence in natural waters in terms of modulation transfer functions using measured turbulence dissipation rates. Image data collected from natural environments during the Skaneateles Optical Turbulence Exercise are presented. Accurate assessments of the turbulence conditions are critical to the model validation and were measured by two instruments to ensure consistency and accuracy. Optical properties of the water column in the field were also measured in coordination with temperature, conductivity, and depth. The results show that optical turbulence degrades the image quality as predicted and on a level comparable to that caused by the particle scattering just above the thermocline. Other contributing elements involving model closure, including temporal and spatial measurement scale differences among sensors and mitigation efforts, are discussed.

15. SUBJECT TERMS
Optical turbulence, ocean optic, imaging underwater turbulence

16. SECURITY CLASSIFICATION OF:			17. LIMITATION OF ABSTRACT	18. NUMBER OF PAGES	19a. NAME OF RESPONSIBLE PERSON
a. REPORT	b. ABSTRACT	c. THIS PAGE			Weilin Hou
Unclassified	Unclassified	Unclassified	UU	09	19b. TELEPHONE NUMBER *(Include area code)* (228) 688-5257

Reset

Standard Form 298 (Rev. 8/98)
Prescribed by ANSI Std. Z39.18

PUBLICATION OR PRESENTATION RELEASE REQUEST

Pubkey: 7807 NRLINST 5600.2

Ref: (a) NRL Instruction 5600.2
(b) NRL Instruction 5510.40D

Encl: (1) Two copies of subject paper (or abstract)

( ) Abstract only, published
( ) Book
( ) Conference Proceedings (refereed)
( ) Invited speaker
(X) Journal article (refereed)
( ) Oral Presentation, published
( ) Other, explain

( ) Abstract only, not published
( ) Book chapter
( ) Conference Proceedings (not refereed)
( ) Multimedia report
( ) Journal article (not refereed)
( ) Oral Presentation, not published

STRN NRL/JA/7330-11-843
Route Sheet No. 7330/
Job Order No. 73-6369-01-5
Classification X U C
Sponsor ONR
approval obtained ___ yes X no

Title of Paper or Presentation

Optical Turbulence on Underwater Image Degradation in Natural Environments

Author(s) Name(s) (*First,MI,Last), Code, Affiliation if not NRL*

Weilin Hou 7333 **Sarah Woods** ASEE **Ewa Jarosz** 7332 **Wesley A. Goode** 7333 **Alan D. Weidemann** 7333

It is intended to offer this paper to the _____
(Name of Conference)

_____
(Date, Place and Classification of Conference)

and/or for publication in **Applied Optics, Unclassified** _____
(Name and Classification of Publication) *(Name of Publisher)*

After presentation or publication, pertinent publication/presentation data will be entered in the publications data base, in accordance with reference (a).
It is the opinion of the author that the subject paper (is ____) (is not ___X) classified, in accordance with reference (b).
This paper does not violate any disclosure of trade secrets or suggestions of outside individuals or concerns which have been communicated to the Laboratory in confidence. This paper (does ____) (does not ___X) contain any militarily critical technology.
This subject paper (has ____) (has never __X__) been incorporated in an official NRL Report.

Weilin Hou, 7333 _____
Name and Code *(Principal Author)* (Signature)

CODE	SIGNATURE	DATE	COMMENTS
Author(s) Hou		9/13/2011	Need by 27 Sep 11
			Publicly accessible sources used for this publication
Section Head Weidemann	TDY		
Branch Head **Robert A Arnone, 7330**		9/13/11	
Division Head **Ruth H. Preller, 7300**		9/13/11	1. Release of this paper is approved. 2. To the best knowledge of this Division, the subject matter of this paper (has ____) (has never __X__) been classified.
Security, Code **1231**			1. Paper or abstract was released. 2. A copy is filed in this office.
Office of Counsel,Code **1008.3**	Kathy Chapman	9/13/11	
ADOR/Director NCST **E. R. Franchi, 7000**			
Public Affairs *(Unclassified/ Unlimited Only)*, Code **7030.4**	Shannon Foreland	9/28/11	
Division, Code			
Author, Code			

HQ-NRL 5511/6 (Rev. 12-98) (e) THIS FORM CANCELS AND SUPERSEDES ALL PREVIOUS VERSIONS

11-1226-3498

PUBLICATION OR PRESENTATION RELEASE REQUEST

Pubkey: 7807 NRLINST 5600.2

Ref: (a) NRL Instruction 5600.2
(b) NRL Instruction 5510.40D

Encl: (1) Two copies of subject paper (or abstract)

( ) Abstract only, published
( ) Book
( ) Conference Proceedings (refereed)
( ) Invited speaker
(X) Journal article (refereed)
( ) Oral Presentation, published
( ) Other, explain

( ) Abstract only, not published
( ) Book chapter
( ) Conference Proceedings (not refereed)
( ) Multimedia report
( ) Journal article (not refereed)
( ) Oral Presentation, not published

STRN NRLJA/7330-11-843
Route Sheet No. 7330/
Job Order No. 73-6369-01-5
Classification X U
Sponsor ONR B&L.2 ns
approval obtained yes X no

Title of Paper or Presentation
Optical Turbulence on Underwater Image Degradation in Natural Environments

Author(s) Name(s) (*First,MI,Last*), Code, *Affiliation if not NRL*

Weilin Hou 7333 **Sarah Woods** ASEE **Ewa Jarosz** 7332 **Wesley A. Goode** 7333 **Alan D. Weidemann** 7333

It is intended to offer this paper to the _____
(Name of Conference)

(Date, Place and Classification of Conference)

and/or for publication in **Applied Optics, Unclassified** _____
(Name and Classification of Publication) *(Name of Publisher)*

After presentation or publication, pertinent publication/presentation data will be entered in the publications data base, in accordance with reference (a).
It is the opinion of the author that the subject paper (is ____) (is not __X__) classified, in accordance with reference (b).
This paper does not violate any disclosure of trade secrets or suggestions of outside individuals or concerns which have been communicated to the Laboratory in confidence. This paper (does ____) (does not __X__) contain any militarily critical technology.
This subject paper (has ____) (has never __X__) been incorporated in an official NRL Report.

Weilin Hou, 7333 ✓
Name and Code (*Principal Author*)

(Signature)

CODE	SIGNATURE	DATE	COMMENTS
Author(s) Hou		9/13/2011	Need by 27 Sep 11
			Publicly accessible sources used for this publication
Section Head Weidemann	TDY		This is a Final Security Review. Any changes made in the document after approved by Code 1226 nullify the Security Review.
Branch Head Robert A Arnone, 7330		9/13/11	1. Release of this paper is approved. 2. To the best knowledge of this Division, the subject matter of this paper (has ____) (has never __X__) been classified.
Division Head Ruth H. Preller, 7300		9/13/11	1. Paper or abstract was released. 2. A copy is filed in this office.
Security, Code 1231		9/20/11	
Office of Counsel,Code 1008.3	Kathy Chapman	10/3/11	Sponsor approval attached
ADOR/Director NCST E. R. Franchi, 7000			
Public Affairs (*Unclassified/ Unlimited Only*), Code 7030.4		9/28/11	
Division, Code			
Author, Code			

HQ-NRL 5511/6 (Rev. 12-98) (e) THIS FORM CANCELS AND SUPERSEDES ALL PREVIOUS VERSIONS

14 SEP '11 PM 2:41

Optical turbulence on underwater image degradation in natural environments

Weilin (Will) Hou[1], Sarah Woods[1,2], Ewa Jarosz[1], Wesley Goode[1], Alan Weidemann[1]

1 Naval Research Laboratory, 1009 Balch Blvd, Stennis Space Center, MS 39529, USA

2 ASEE NRL Post Doctoral Fellow

Corresponding author: hou@nrlssc.navy.mil

It is a well-known fact that the major degradation source on electro-optical (EO) imaging underwater is from scattering by the medium itself and the constituents within, namely particles of various origins and sizes. Recent research indicates that under certain conditions, the apparent degradation could also be caused by the variations of index of refraction associated with temperature and salinity micro-structures in the ocean and lakes. These would inherently affect the optical signal transmissions underwater, which is of vital interest to both civilian and military applications, as they could include diver visibility, search and rescue, mine detection and identification, and optical communications. The combined impact has been modeled previously through the Simple Underwater Imaging Model (SUIM). The current study presents the first attempts in quantifying the level of EO image degradation due to optical turbulence in natural waters, in terms of modulation transfer functions. Image data collected from natural environments during the Skaneateles Optical Turbulence Exercise (SOTEX, July 22-31, 2010) using the Image Measurement Assembly for Subsurface Turbulence (IMAST) are presented. Accurate assessment of the

turbulence conditions are critical to the model validation, and were measured by two different approaches, namely a 3D Doppler based velocimeter with the conductivity and temperature combo, and a shear based Vertical Microstructure Profiler. The results are compared to ensure consistency and accuracy, under different deployment configurations. Optical properties of the water column in field were measured using WETLab's ac-9 and Sequoia's LISST (Laser In Situ Scattering and Transmissiometry), in coordination with temperature, conductivity and depth. The results show that optical turbulence degrades the image quality on a level similar to that caused by the particle scattering. Several contributing elements involving model closure, including measurement temporal and spatial scale differences amongst sensors, and mitigation efforts are discussed, along with plans on future research.

OCIS codes: 010.4450, 010.7060, 010.7295.

1. Background

When it comes to diver visibility, the most prominent issue is the degradation of image quality over distance due to attenuation. This presents a striking contrast for us who are used to the seemingly unlimited visual ranges in air. The cause of the degradation has been mostly attributed to the "dirt", or inorganic as well as organic particles (ie micro-organisms and detritus) in the water and it is rightly so. Most research has focused on reducing the impact of particle scattering by means of discriminating scattering photons involving polarization, range gating, modulation, and by means of restoration via deconvolution [1-6]. However, in clean oceanic or lake waters, another factor could come into play to the effects of the same order. This is the scattering by optical turbulence, which is caused by variations of the index of refraction of the medium. This is

mostly associated with the turbulence structures of the medium, or water body in our case. Degradation of the image quality in a scattering medium involving turbulence has been studied mostly in atmosphere [7-9]. These studies are mainly focused on modeling the optical transfer function as a function of density variation by association with wind profiles, in an effort to restore the images obtained, such as in air reconnaissance or astronomy studies [10, 11]. Little has been done regarding the turbulence effects on imaging formation in water, mainly due to the dominant particle scattering and associated attenuation. This is of little surprise to anyone with experience in coastal waters, especially those inside a harbor, or estuarine areas like Mississippi, where visibility could quickly reduce to zero in a matter of a few feet. The same applies to regions of strong re-suspension from the bottom, both in coastal regions as well as in the deep sea. The effects of turbulence have been postulated to have impacts over long image transmission range [12], which has been supported by light scattering measurements and simulations [13]. Under extreme conditions, observations have been made that involve targets with a pathlength of a few feet [14]. The images obtained under such conditions are often severely degraded or blurred, on par with or more than those caused by particle scattering. Overcoming such challenges to increase both the reach and the resolution is important to current and future underwater EO applications, from mine detection and identification, to diver visibility, pipe inspection, undersea communications, as well as search and rescue operations. It is critical to establish a good understanding about the limiting factors under different conditions. SUIM [15] was developed to address this issue and it has been shown in theory that, on average, the relative contribution of different components [3, 16] in underwater imaging applications can be expressed in terms of the optical transfer function (OTF) as

$$
\begin{aligned}
OTF(\psi,r)_{total} &= OTF(\psi,r)_{path}\,OTF(\psi,r)_{par}\,OTF(\psi,r)_{tur} \\
&= \left(\frac{1}{1+D}\right)\exp\left[-cr + br\left(\frac{1-e^{-2\pi\theta_0\psi}}{2\pi\theta_0\psi}\right)\right]\exp\left(-S_n\psi^{5/3}r\right) \qquad (1)\\
&= \left(\frac{1}{1+D}\right)\exp\left\{-\left[c - b\left(\frac{1-e^{-2\pi\theta_0\psi}}{2\pi\theta_0\psi}\right) + S_n\psi^{5/3}\right]r\right\}
\end{aligned}
$$

where θ_0 relates to the mean scattering angle, c and b are the beam attenuation and scattering coefficients respectively. Ψ is the spatial frequency in cycles per radian, r is the imaging range, and D relates to path radiance [3]. S_n contains parameters that are dependent on the structure function and which can be further expressed in terms of the turbulence dissipation rate of temperature, salinity and kinetic energy, assuming Kolmogorov power spectrum type.

$$S_n = 3.44(\bar{\lambda} / R_0)^{5/3} = 1736K_3\bar{\lambda}^{1/3} \qquad (2)$$

where K_3=$B_1\chi\varepsilon^{-1/3}$, and reflects the 3-dimensional optical turbulence strength. $\bar{\lambda}$ is the average wavelength of the transmitted light. R_0 is the characteristic seeing parameter [15]. B_1 is a constant, and assumed to be on the order of unity [17]. The kinetic energy dissipation rate (TKED, ε), typically ranges from 10^{-3} to 10^{-11} m^2s^{-3} in natural waters. χ relates to the dissipation rate of temperature (TD) or salinity variances [17].

Since the phase information can be ignored under incoherent imaging conditions, the magnitude of the OTF or the modulation transfer function (MTF) will be used interchangeably here. The above model has been checked using indirect measurements, without involvement of direct field turbulent measurements, nor with a stable imaging platform to obtain underwater imagery. These issues are addressed by our recent field efforts, which are presented in this paper. We will discuss our field exercise in the next section, followed by the section on image acquisition and SUIM model validation. Lastly, we discuss issues related to model and measurement accuracy, applicability and improvements.

2. SOTEX

2.1 Experiment site

Optical turbulence underwater is primarily a function of temperature structure, although salinity variations could at times contribute to strong optical turbulence [14]. Intensified thermoclines in natural environments provide a convenient setup to examine this chaotic process. We identified one of the Finger Lakes in upstate New York, Skaneateles, as our test site for SOTEX (Skaneateles Optical Turbulence EXercise, July, 2010). Figure 1 shows the approximate location of the two stations, the first (S1, red circle) near the center of the lake (42.8668^{o} N, 76.3920^{o} W) over a sloping bottom with an approximate depth of 70m, the second (S2, blue triangle) at the northern end of the lake (42.9063^{O} N, 76.4058^{O} W) over a flatter bottom with an approximate depth of 50m. The lake is the clearest of all finger lakes, with an average Secchi depth near 8m [18], and allowing for imaging under varied turbulent strength, while with little scattering contribution from particulates. The strong stratification in July at relatively shallow depth, with less wind and current interference ensures a well-defined thermocline, as demonstrated by the temperature profile shown in Figure 2, measured by a PME CT sensor. The same features help to form strong structures for optical turbulence in the lake. The optical properties of the water column were measured by a 9-channel absorption and attenuation meter (ac-9, by WETLabs), and Laser In Situ Scattering Transmissometer (LISST, Sequoia Scientific). We notice that the water in the top part of the water column, just above the sharp thermocline, until about 9m, is typically rather clear, with beam attenuation at 532nm valued below 0.4m^{-1}, before increasing sharply for the day shown (July 27, Fig.2). The LISST data is primarily used to estimate the point spread function (PSF) of the water, which can be used for image model

restoration [16], as well as estimation of MTF. This effort will be discussed in a separate publication.

2.2 Instrumentation and Measurements

In order to estimate the effects of the optical turbulence in the water column, it is essential to remove any other variations that could contribute to the blurring of the imagery obtained. For this reason, the Image Measurement Assembly for Subsurface Turbulence (IMAST) was designed and implemented at NRL (Fig. 3). The camera and housing, passive and active imaging targets are attached to the 5m aluminum structure, along with the Vector, and a CTD. A separate optical profiler frame containing the optical sensors discussed above is deployed in close vicinity of the IMAST, under the assumption of homogeneity.

The SUIM model requires accurate assessments of turbulence structures, of both the rates of TKED, ε, and TD, χ. Two sets of instrumentation were used to make these observations, to maximize their applicability to our needs. The first instrumental setup, the Vector/CT, consists of a Nortek Vector acoustic Doppler 3D velocimeter and a Precision Measurements Engineering (PME) fast Conductivity and Temperature (CT) sensor. The two instruments are mounted near the center of the IMAST structure, and the heads of the instruments placed in such a way as to sample the same volume of water, thus providing time series of the 3D velocity, temperature, and conductivity fluctuations of the sample water volume. As the instrument is commonly used for laboratory measurements or stationary moorings, the instrument requires collection of a time series of velocities at a stationary depth in order to compute the turbulent dissipation rates. Therefore, during deployment, the IMAST profiled the water column by pausing at each depth for five to fifteen minutes to capture the turbulence statistics. The second turbulence instrument,

providing microstructure observations for SOTEX, is the VMP. It is equipped with four microstructure sensors: two shear sensor probes, one thermistor (FP07), and micro-conductivity (SBE7) sensor. These sensors allow measuring with high accuracy and resolution microscale velocity shear, temperature, and conductivity. Additionally, the VMP profiler has externally attached SeaBird SBE7-3F temperature and SBE-4C conductivity sensors..

Two sets of instrumentation were utilized for characterizing the turbulence strength during SOTEX in order to provide a comparison between the background turbulence of the lake and the turbulence within the IMAST, to ensure the IMAST itself was not inducing significant turbulence. This setup is necessary, as we want to have optical turbulence measured during the imaging process. The free-falling deployment nature of the VMP is not suitable for our needs, despite its high temporal sampling rate and maturity in technology in terms of quantifying underwater turbulence. The compactness of Vector/CT setup is ideal for our application. However, it is not designed for turbulence profiling and a comparison or inter-calibration is necessary. Details of the turbulence measurements methods and results may be found in [19].

To keep the IMAST to a manageable size and weight for ease of deployment, the imaging system, the target and the environmental characterization sensors are all made to be self-contained. Besides a reflective custom-made resolution chart set, an active target is made utilizing an iPad for active illumination, displaying a standard USAF 1951 chart in order to reduce the effects of path radiance. A commercial off the shelf (COTS) high speed imaging camera by Casio (EX-F1) is used to record images at various frame rates, up to 300 fps at 500x400 pixels, and higher resolution with reduced frame rates including native full HD resolution (1920x1080 pixels). As only the relative contrasts of different spatial frequencies are needed, we ignore the irradiance variations from the targets, or exposure settings on the camera,

so long as they remain fixed and constant during each cast. IMAST is deployed in two configurations in the water column, vertical and horizontal. In the horizontal mode, the frame is suspended in the water column, in the middle of, above and beneath the thermocline for extended periods of time, in order to accurately quantify the turbulence environment (Fig. 4).

It is understandable that the IMAST would introduce drag and affect turbulence flow. However, since we are measuring the turbulence in situ, along the imaging path, it should not introduce significant errors to bias our validation.

3. Results and Model Validation

The impact of optical turbulence becomes obvious when a pair of sample images is examined side by side (Figure 5), one with strong optical turbulence and one without, under similar turbidity conditions. They are taken at two different depths, one at 2.8m which is essentially free of optical turbulence, while the one at 8.7m is strongly influenced by optical turbulence. This is a reasonable assumption, even though we do not have TD rates measured at 2.8m [20]. From the temperature profiles shown in Fig. 2, one should expect neglectable amount of optical turbulence at the shallow depths where temperature profile is essentially uniform, thus reflected in very low TD rates. Both images are taken under the horizontal deployment configuration. One can notice that despite of the similar optical properties measured (beam c less than $0.4m^{-1}$, Fig.2), the one inside the strong turbulence layer (b) suffered much more degradation, compared to the weaker turbulence situation (a). It is worth mentioning that for the IMAST-iPad setting, the 0-2 group of the USAF 1951 resolution chart corresponds to the spatial frequency of 1900 cyc/rad or 1.9 cyc/mrad.

There are many ways to quantify such degradation. The most direct way, and also to work directly with SUIM is to estimate the image degradation in terms of the MTF, which describes the total system response at different spatial frequencies. Granted, this might not be the best approach for turbulence degraded images, especially under high levels of distortion. However, we intend to estimate the long exposure (averaged) impacts, and such an approach is acceptable for this purpose. There are several methods to derive the MTF from imagery. We choose a standard slant edge technique [21, 22] by measuring the corresponding frame-averaged MTF.

To test our hypothesis that the difference in image quality is caused by optical turbulence, we checked the single frame MTF against multi-frame-averaged MTF. The results show that there is very little difference under the weak turbulence situation, but noticeable differences in the stronger turbulence case (Figure 6), which confirms our hypothesis, at least to the first order.

From SUIM, we can see that if we assume the path radiance is the same, which is the reason for conducting the night deployment with an active target, and we also assume the particulate scattering characteristics, including single scattering albedo, ω_o, and mean scattering angle, are the same at the depths we are interested in, then the difference of the MTF at depth 2 (H_2) relative to depth 1 (H_1) can be written as

$$H_2(\psi, r) = \exp[-(S_{n2} - S_{n1})\psi^{5/3} r] \bullet \exp[-(c_2 - c_1)(1 - \varpi_0(\frac{1 - e^{-2\pi\theta_0\psi}}{2\pi\theta_0\psi})] \bullet H_1(\psi, r) \qquad (3)$$

where S_{n2} and S_{n1} are optical turbulence intensity at the corresponding depths, respectively.

From Eq. (3), we can calculate MTFs from the depth of 8.7m based on measured turbulence dissipation rates from the Vector and the VMP, to estimate the impacts from optical turbulence. The results are shown in Figure 7 (a-d). These are obtained from an active source (one way path) during the night deployment of July 27, to minimize path radiance. Fig. 10a

shows the averaged MTF at the shallower depth (2.8m), compared to several cases (sequences A, B, and C as marked) at the deeper depth (8.7m) where optical turbulence is strong. For each of the image sequences at 8.7m, the MTFs are estimated using the same region of interest (ROI) of consecutive frames, over 10-frames for long exposure, to be compared to the single-frame, and averaged-frame results at 2.8m, as well as modeled outcome. As explained above, the averaging and comparison to single frame results at 2.8m is used to examine the level of degradation over longer exposure. The SUIM model [15, 23] is used to incorporate the impacts of optical turbulence at 8.7m, using different turbulence parameters for each sequence with R_0 =0.0045, 0.006, 0.008m^{-1}. These values are calculated with Eq. 2 using measured TKED and TD rates [20] as $\varepsilon=10^{-7}$, 10^{-9}, $10^{-9.2}$, $\chi=10^{-6}$, $10^{-6.4}$, $10^{-6.3}$, respectively. It is worth noting that the signal to noise ratio (SNR) cannot be improved when multiple frames are used, as each individual frame would typically undergo a different amount of degradation. Therefore the averaging would only increase the SNR towards the low frequency elements, and leave behind random variations at the high frequency end. This is necessary, however, in order to contain all of the variations caused by the optical turbulence [15].

4. Discussion

One should bear in mind that even under turbid conditions, optical turbulence still affects image quality, although the relative contribution would be small. Although this is evident from Eq. 1, intuitively it is not necessarily the case which is the primary reason behind this paper. By applying TKED rates of 10^{-7}~10^{-9} m^2s^{-3}, and temperature dissipation rates of 10^{-6}~10^{-7} $^oC^2s^{-1}$, one can see that the model result approximates the field measurements reasonably well. It is understandable that the model cannot be applied in all situations, and should not expect to fully

explain every details of measurements, considering the challenges involved in quantifying turbulence for IMAST [20]. It would be beneficial, therefore, to examine the discrepancies for the purpose of improvements in model as well as measurements.

The differences between the model and measurements could be the result of myriad factors. The primary reason is likely the difference in measurement scales in the temporal domain. In other words, the amount of time needed to measure the turbulence structure, both TKED and TD , is much longer, as compared to EO processes. This is understandable, as the only way to quantify chaotic processes is to use statistical approach, which takes time and space for enough sampling points in order to eliminate impacts from random fluctuations. This is troublesome, especially when spatial fluctuations of the turbulent flow cannot be treated as isotropic, nor statistically homogenous. This uncertainty caused by measurement mismatch will prevent a more in-depth understanding of the process involved, thus hindering efforts to mitigate the impacts. In theory, short exposure method can be used to freeze the impacts for restoration, similar to those done in astronomy. However, it is very difficult to determine whether nearby distortions are from the same isoplanatic patch, when relatively few data samples are available. Highly complex iterative methods are under development, in order to compensate or reduce the degradation [24]. Because of this limitation, the best one can do for the model validation is probably using a thru-the-sensor approach, and range check as we have done here. In other words, due to the incompatibility in temporal scale measurements, we could not expect to pin-point an exact value in TKED and TD rates, but can only rely on the range of values. An instantaneous assessment of turbulence strength across the imaging path is highly desirable, which might stem from the success of the scintillation approach in astronomy and optical

communications [25]. More rigorous post-processing of images involving multiple ROIs, and direct derivation of MTFs using the whole resolution pattern should help to improve the results.

Another limitation of this method is the inconsistency in measurement scales between optical properties of the medium and the imaging path under examination, both temporally and spatially. It has been pointed out that due to the sample volume limitations of most in situ optical sensors, including the traditional beam-c meters, recently instruments like ac-9 and LISST, one cannot obtain a meaningful, complete picture of the particle suites that exist along the entire imaging path [26]. In our SOTEX setup, the number of larger particles (>50μm) within the few cubic centimeters of the sample volume of the ac-9 is next to none, over its sampling time. While in the mean time, the imaging path of IMAST would include an equivalent sample volume at least 10^4 times larger. This, in turn, implies a significant bias when the optical properties from ac-9 are used [26]. This is an inherent flaw to this approach and can be addressed by a different measurement approach, likely involving new instrumentation not readily available short term. Alternatively, with thorough knowledge of the instruments (transmission optics, sensor acceptance angle), and in situ particle size distribution obtained over large or at least equivalent sample volume, one could theoretically estimate the bias, given particle composition or assuming the ranges of index of refractions. This is, however, beyond the scope of this paper.

Nevertheless, we can carry out a quick investigation by examining the impacts and see if the above hypothesis is correct. We ran the SUIM with a different set of beam-c values, thus different particulate scattering, to see if the model differences shown in Fig. 7 can be reduced. The results are shown in Figure 8, for the three cases (A, B and C) examined earlier. By introducing the amount of “excessive” scattering ranging from 0.16~0.2m^{-1}, a closer fit can be

achieved. Additionally, this also suggests that there might exist discrepancies between the time-invariant beam-c measurements versus the time-varying degradations from the turbulence.

Lastly, our analysis of underwater images of beam propagation suggest particle scattering and turbulence is likely a coupled process, especially under turbid conditions. Efforts are underway to investigate and model such contributions.

5. Conclusion

The impact of optical turbulence on imaging is directly measured in the field for the first time during our SOTEX exercise in July 2010, with both optical properties and turbulence dissipation rates quantified. This paper presented direct evidences of image degradation by optical turbulence in natural environment, under similar turbidity conditions. By quantifying the degradation and field turbulent conditions through TKED and TD rates, and optical conditions through absorption and scattering, we achieved closure by partitioning image degradation to particle scattering and turbulence scattering, respectively. Results showed that directly measured MTFs over turbulent flow using slant edge method from the field obtained images matched well with model derived MTFs based on turbulence model. The discrepancies can be attributed to factors associated with differences in measurement scales in both temporal and spatial domains. Efforts are underway to investigate more complex turbulence conditions involving dissipations from both temperature and salinity variations in the ocean. Algorithms are also being developed to mitigate impacts of optical turbulence on image degradation.

Acknowledgement

This research was supported by ONR program element 62782N (NRL core project 73-6369). The authors thank the scientists and staff at the Upstate Freshwater Institute (UFI) for their assistance throughout SOTEX.

References

1. G. D. Gilbert, and J. C. Pernicka, "Improvement of underwater visibility by reduction of backscatter with a circular polarization technique," Appl. Opt. **6**, 741-746 (1967).

2. W. Hou, A. Weidemann, D. Gray, and G. R. Fournier, "Imagery-derived modulation transfer function and its applications for underwater imaging," in *Applications of Digital Image Processing XXX*, A. G. Tescher, ed. (SPIE, San Diego, 2007), pp. 6696221-6696228.

3. W. Hou, Z. Lee, and A. Weidemann, "Why does the Secchi disk disappear? An imaging perspective," Opt. Express **15**, 2791-2802 (2007).

4. P. C. Chang, J. C. Flitton, K. I. Hopcraft, E. Jakeman, D. L. Jordan, and J. G. Walker, "Improving visibility depth in passive underwater imaging by use of polarization," Appl. Opt. **42**, 2794-2803 (2003).

5. L. Mullen, A. Laux, B. M. Concannon, E. P. Zege, I. L. Katsev, and A. S. Prikhach, "Amplitude-modulated Laser Imager," Appl. Opt. **43**, 3874-3892 (2004).

6. G. R. Fournier, D. Bonnier, J. L. Forand, and P. W. Pace, "Range-gated underwater laser imaging system," Optical Engineering **32** (1993).

7. D. L. Fried, "Optical resolution through a randomly inhomogeneous medium for a very long and very short exposures," J. Opt. Soc. Am. **56**, 1372-1379 (1966).

8. M. C. Roggemann, and B. M. Welsh, *Imaging through turbulence* (CRC Press, 1996).

9. N. Kopeika, "Imaging through the atmosphere for airborne reconnaissance," Optical Engineering **26**, 1146-1154 (1987).

10. D. Sadot, A. Dvir, I. Bergel, and N. Kopeika, "Restoration of thermal images distorted by the atmosphere, based on measured and theoretical atmospheric modulation transfer function," Optical Engineering **33**, 44-53 (1994).

11. Y. Yitzhaky, I. Dror, and N. Kopeika, "Restoration of atmospherically blurred images according to weather-predicted atmospheric modulation transfer functions," Optical Engineering **36**, 3062-3072 (1997).

12. W. H. Wells, "Theory of small angle scattering," in *AGARD Lec. Series No. 61*(NATO, 1973).

13. D. J. Bogucki, J. A. Domaradzki, R. E. Ecke, and C. R. Truman, "Light scattering on oceanic turbulence," Appl. Opt. **43**, 5662-5668 (2004).

14. G. D. Gilbert, and R. C. Honey, "Optical turbulence in the sea," in *Underwater photo-optical instrumentation applications.* (SPIE, 1972), pp. 49-55.

15. W. Hou, "A simple underwater imaging model," Opt. Lett. **34** (2009).

16. W. Hou, D. Gray, A. Weidemann, and R. Arnone, "Comparison and validation of point spread models for imaging in natural waters," Opt. Express **16**, 9958-9965 (2008).

17. G. K. Batchelor, "Small-scale variation of convected quantities like temperature in turbulence fluid," J. Fluid Mech. **5**, 113-133 (1959).

18. S. W. Effler, A. R. Rrestigiacomo, and D. M. O'Donnel, "Water quality and limonological monitoring for Skaneateles Lake: Field Year 2007," (Upstate Freshwater Institute, 2008), p. 57.

19. S. Woods, W. Hou, E. Jarosz, W. Goode, and A. Weidemann, "Measurements of turbulence dissipation in Lake Skeneateles," Limnol. Oceanogr. **to be submitted** (2011).

20. S. Woods, W. Hou, W. Goode, E. Jarosz, and A. Weidemann, "Quantifying turbulence microstructure for improvement of underwater imaging," in *Ocean Sensing and Monitoring, SPIE Defense and Security Symposium*, R. A. W. Hou, ed. (SPIE, Orlando, FL, 2011).

21. I. A. Cunningham, and A. Fenster, ""A method for modulation transfer function determination from edge profiles with correction for finite-element differentiation," Med. Phys. **14** (1987).

22. ISO, "ELECTRONIC STILL PICTURE IMAGING SPATIAL FREQUENCY RESPONSE (SFR) MEASUREMENTS," (International Organisation for Standarisation, 1997).

23. W. Hou, S. Woods, W. Goode, E. Jarosz, and A. Weidemann, "Impacts of optical turbulence on underwater imaging," in *Ocean Sensing and Monitoring, SPIE Defense and Security Symposium*, R. A. W. Hou, ed. (SPIE, Orlando, FL, 2011), p. 8.

24. A. Kanaev, W. Hou, and S. Woods, "Multi-frame Underwater Image Restoration," in *SPIE Defense and Security Europe*(SPIE, Prague, Cz, 2011).

25. G. Potvin, J. L. Forand, and D. Dion, "Some theoretical aspects of the turbulent point-spread function," Appl. Opt. **24**, 2932-2942.

26. W. Hou, "Characteristics of large particles and their effects on submarine light field," in *College of Marine Science*(University of South Florida, 1997), p. 149.

Caption

Figure 1. Bathymetric sketch of Skaneateles Lake showing the approximate location of the two stations: S1 (red circle) near the center of the lake, and S2 (blue triangle) in the northern end of the lake. Map from http://www.ourlake.org/html/skaneateles_lake1.html.

Figure 2. Optical properties (beam-c at 532nm) and temperature profile measured during July 27 daytime IMAST deployment. Temperature profiles from other deployments are plotted as well, to show stable and strong thermoclines at Station 1.

Figure 3. IMAST night deployment configuration: imaging camera and housing (left end of the frame); active target made out of iPad (right end of the frame). Notice the Vector and CT locations. Details on other sensors including Vector refer to text.

Figure 4. Diagram of deployment setup showing alternate deployment configurations: Vector/CT deployed on IMAST both vertically and horizontally. Note, in both instances, the VMP was deployed from a separate vessel. The inter-comparison is necessary in order to measure turbulence impacts during IMAST deployments.

Figure 5. Sample image pair obtained by IMAST during night deployment (IMAST horizontal) of July 27. The corresponding physical conditions can be seen in Fig. 2 and related publications (see text). The left (a) was taken at 2.7m depth with no obvious optical turbulence, while the right (b) was from 8.7m, under similar turbidity but strong optical turbulence. They share the same imaging path, camera and light settings. For the current IMAST setting, the 0-2 group corresponds to 1900 cyc/rad.

Figure 6. Normalized MTF of individual (light dashed) and 10-frame averaged (solid line) frame obtained under strong (8.7m) and weak (2.8m) optical turbulent environment during SOTEX. MTFs are calculated using slant edge algorithms over same ROI for all images. The optical properties (particle scattering) of these images are similar, and can be seen in Fig.2

Figure 7. Modulation transfer functions (MTFs) of three different image sequences estimated from 8.7m using the slant edge method, and compared to the modeled results, during July 27 night deployment.

Figure 8. Modulation transfer functions (MTFs) of three different image sequences estimated from 8.7m using the slant edge method, and compared to the modeled results which included extra particle scattering contributions, during July 27 night deployment.

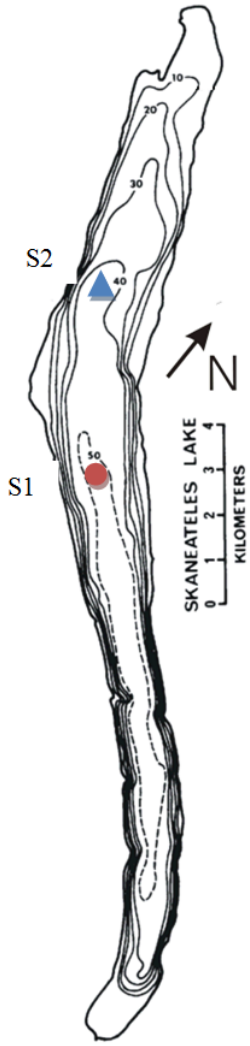

Figure 1. Bathymetric sketch of Skaneateles Lake showing the approximate location of the two stations: S1 (red circle) near the center of the lake, and S2 (blue triangle) in the northern end of the lake. Map from http://www.ourlake.org/html/skaneateles_lake1.html.

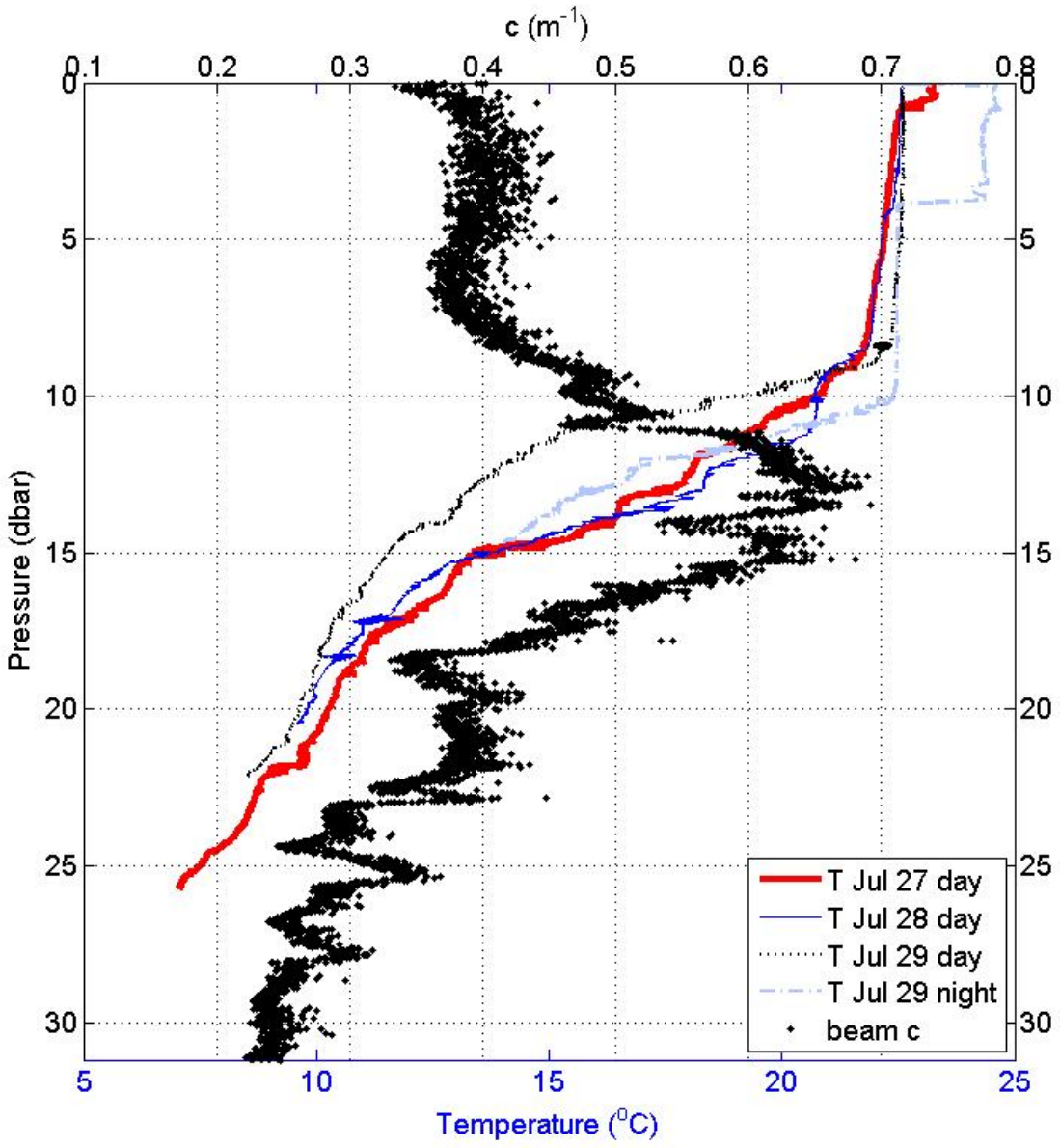

Figure 2. Optical properties (beam-c at 532nm) and temperature profile measured during July 27 daytime IMAST deployment. Temperature profiles from other deployments are plotted as well, to show stable and strong thermoclines at Station 1.

Figure 3. IMAST night deployment configuration: imaging camera and housing (left end of the frame); active target made out of iPad (right end of the frame). Notice the Vector and CT locations. Details on other sensors including Vector refer to text.

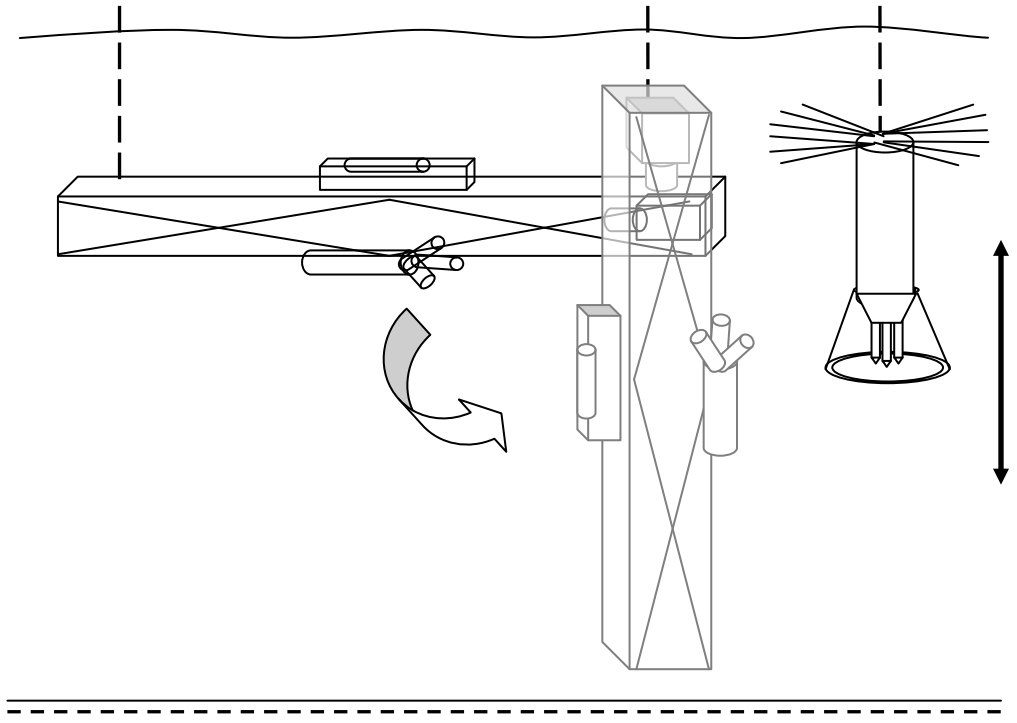

Figure 4. Diagram of deployment setup showing alternate deployment configurations: Vector/CT deployed on IMAST both vertically and horizontally. Note, in both instances, the VMP was deployed from a separate vessel. The inter-comparison is necessary in order to measure turbulence impacts during IMAST deployments.

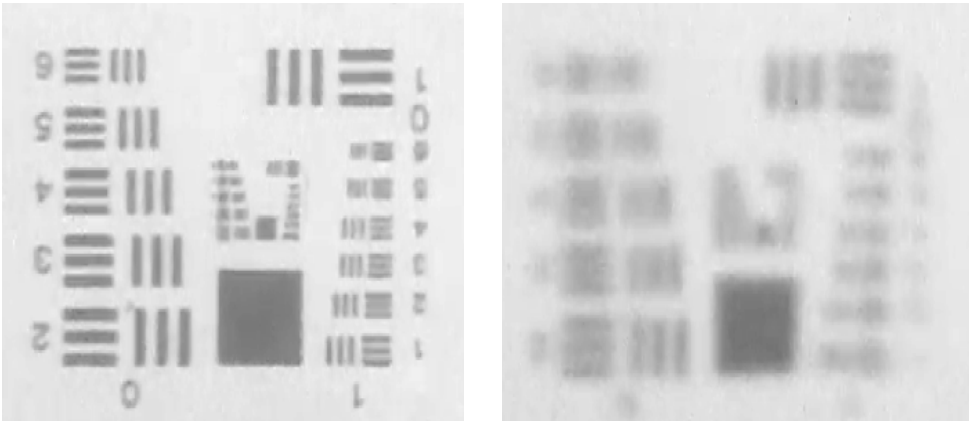

Figure 5. Sample image pair obtained by IMAST during night deployment (IMAST horizontal) of July 27. The corresponding physical conditions can be seen in Fig. 2 and related publications (see text). The left (a) was taken at 2.7m depth with no obvious optical turbulence, while the right (b) was from 8.7m, under similar turbidity but strong optical turbulence. They share the same imaging path, camera and light settings. For the current IMAST setting, the 0-2 group corresponds to 1900 cyc/rad.

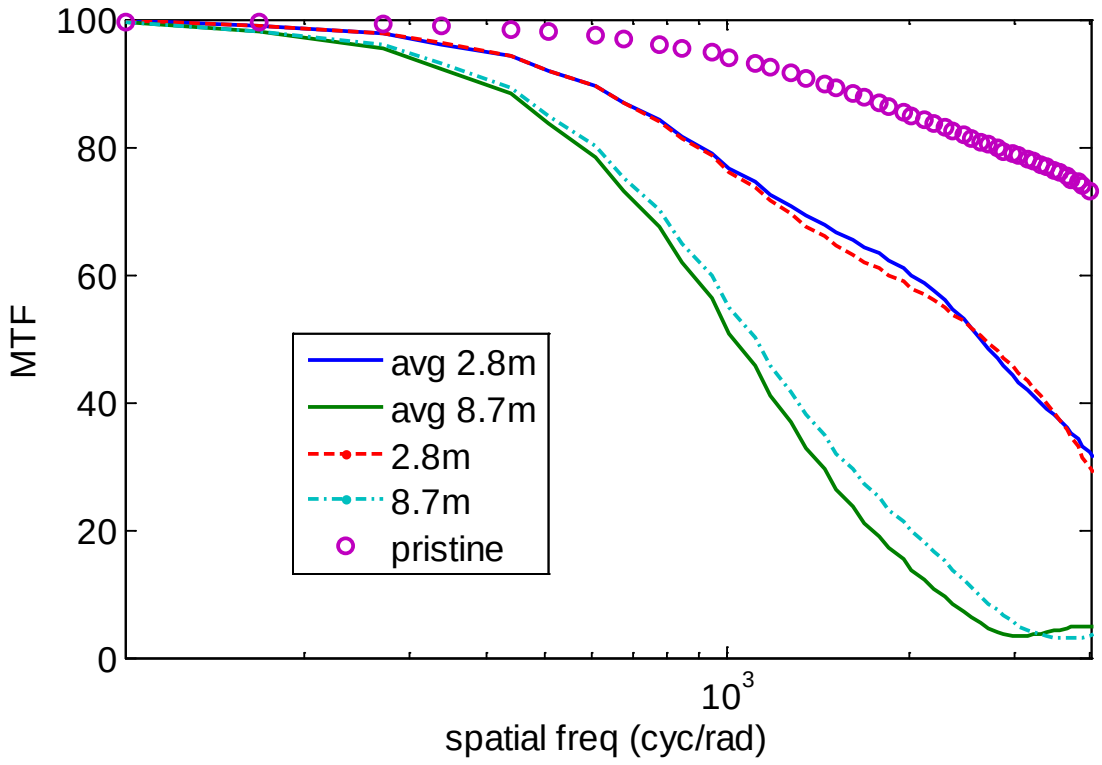

Figure 6. Normalized MTF of individual (light dashed) and 10-frame averaged (solid line) frame obtained under strong (8.7m) and weak (2.8m) optical turbulent environment during SOTEX. MTFs are calculated using slant edge algorithms over same ROI for all images. The optical properties (particle scattering) of these images are similar, and can be seen in Fig.2

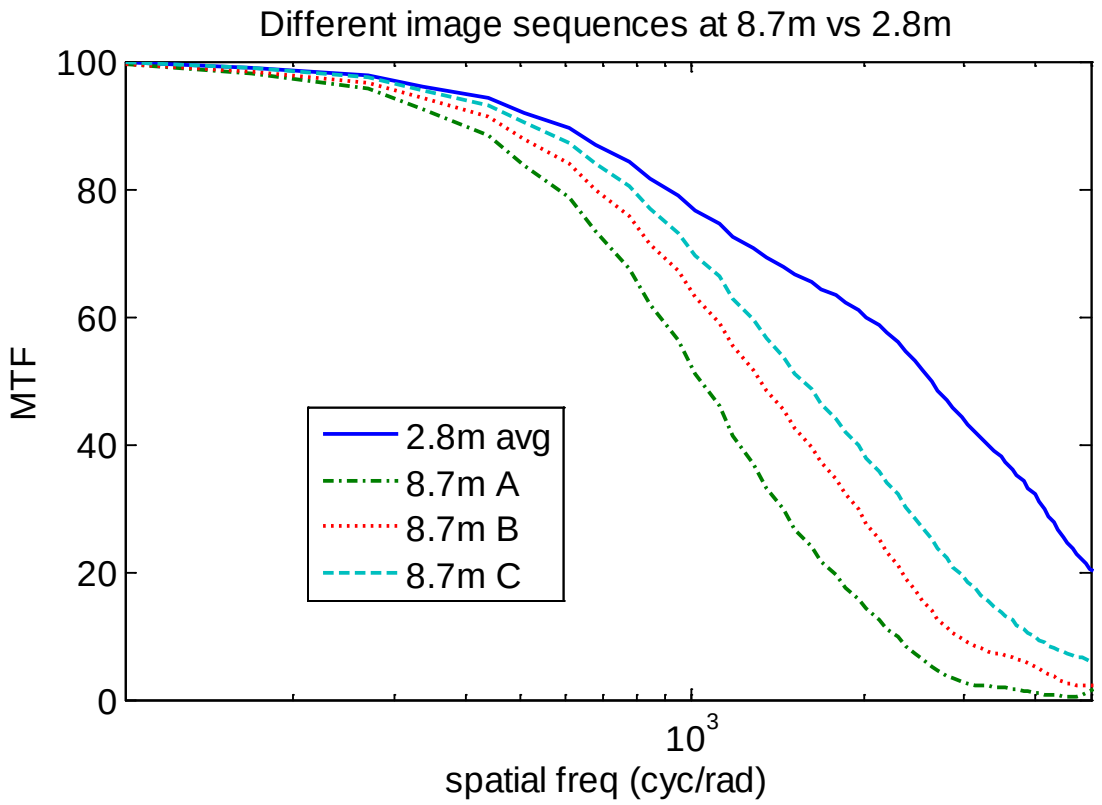
Different image sequences at 8.7m vs 2.8m
MTF
100
80
60
40
20
0
2.8m avg
8.7m A
8.7m B
8.7m C
10^3
spatial freq (cyc/rad)

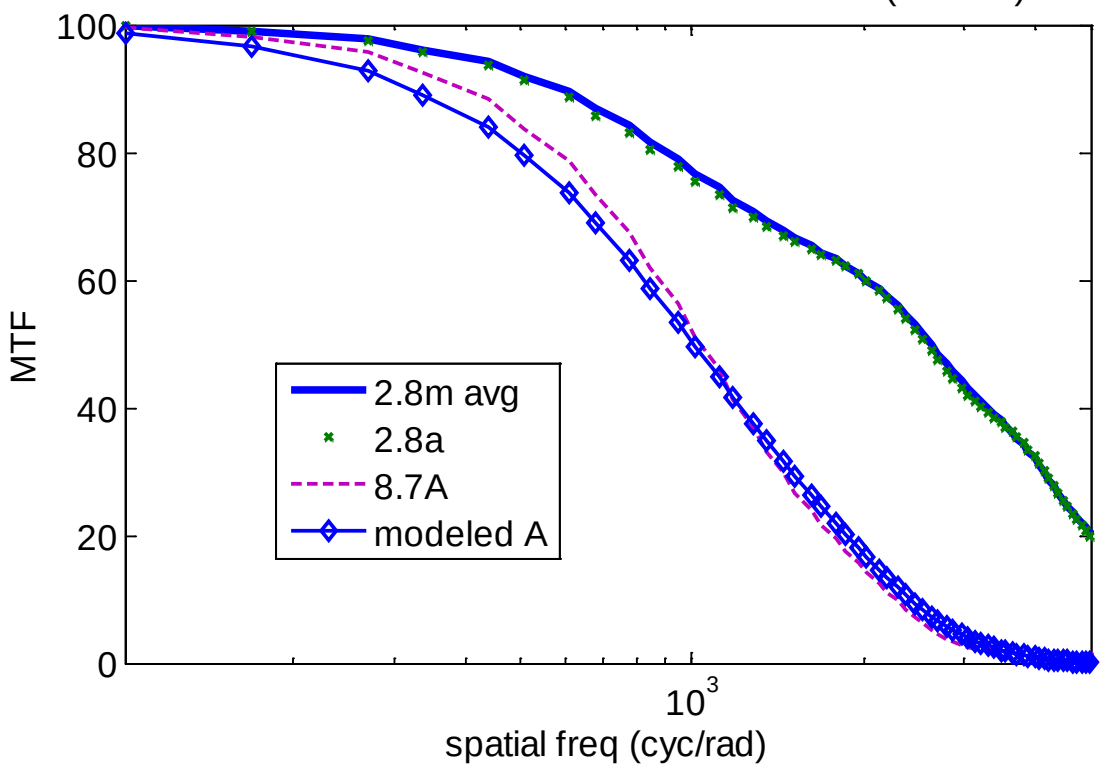
modeled at 8.7m vs measurements at 8.7m (Case A)
MTF
100
80
60
40
20
0
2.8m avg
2.8a
8.7A
modeled A
10^3
spatial freq (cyc/rad)

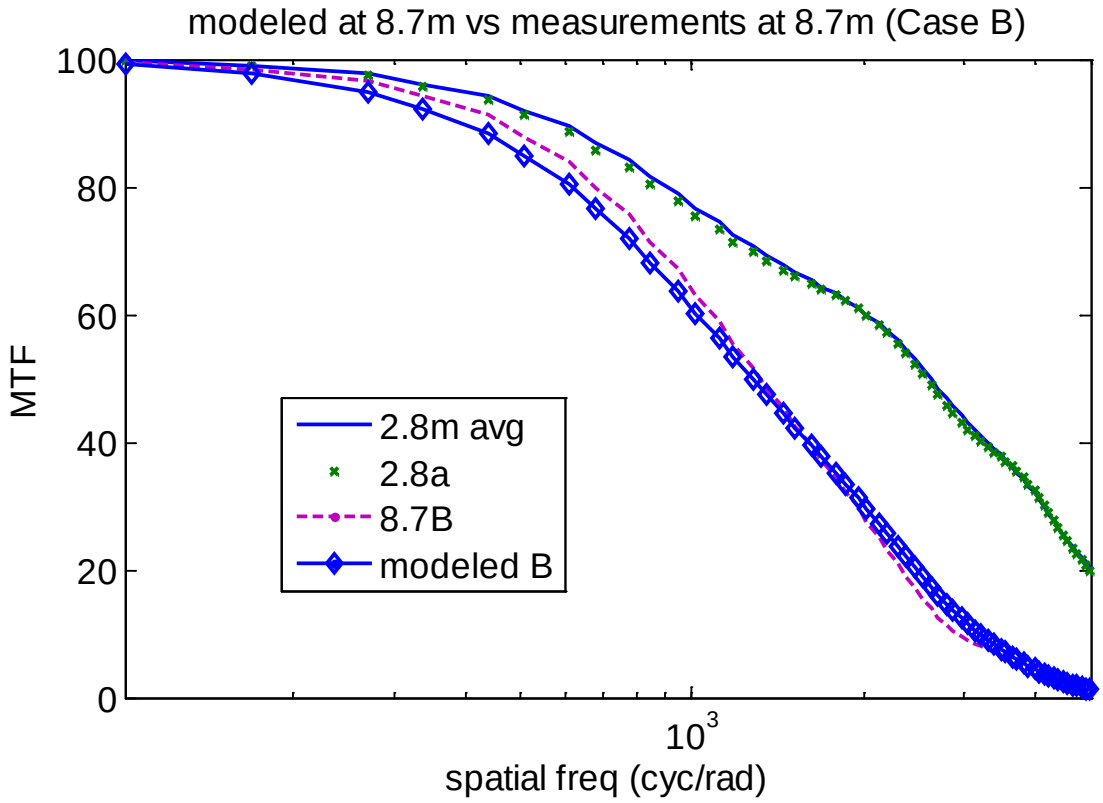
modeled at 8.7m vs measurements at 8.7m (Case B)
100
80
60
40
20
0
MTF
2.8m avg
2.8a
8.7B
modeled B
10^3
spatial freq (cyc/rad)

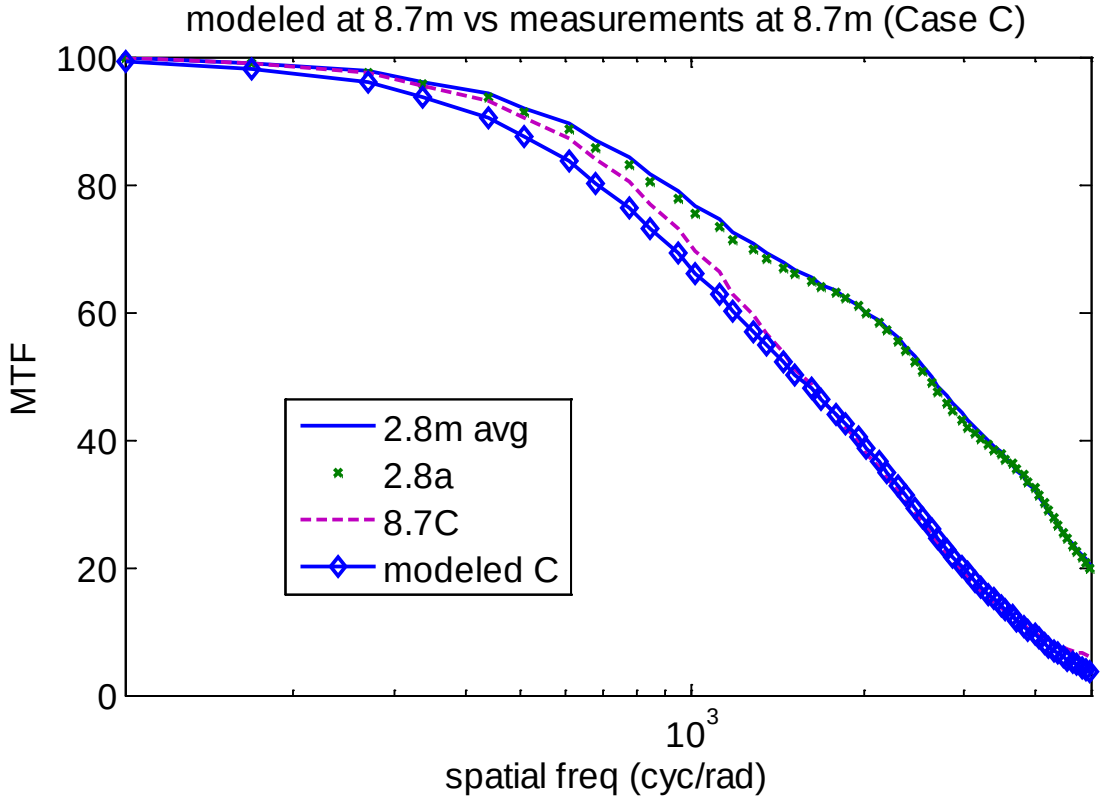
modeled at 8.7m vs measurements at 8.7m (Case C)
100
80
60
40
20
0
MTF
2.8m avg
2.8a
8.7C
modeled C
10^3
spatial freq (cyc/rad)

Figure 7. Modulation transfer functions (MTFs) of three different image sequences estimated from 8.7m using the slant edge method, and compared to the modeled results, during July 27 night deployment.

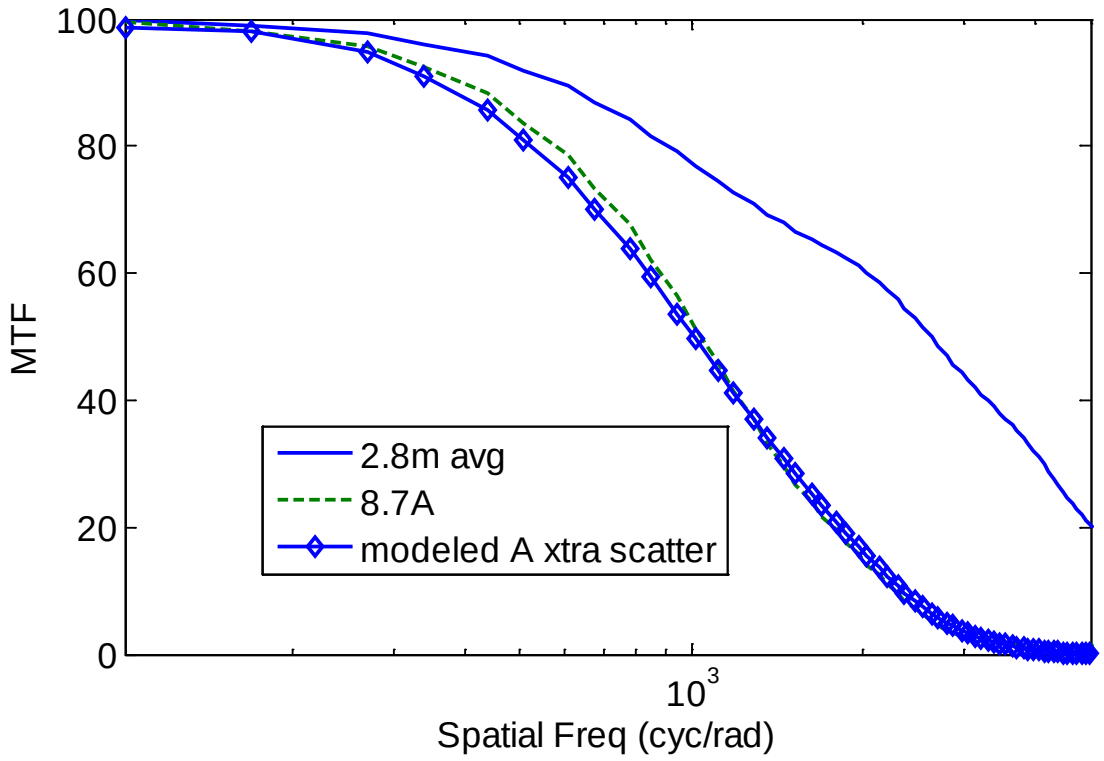
100
80
60
40
20
0
MTF
2.8m avg
8.7A
modeled A xtra scatter
10^3
Spatial Freq (cyc/rad)

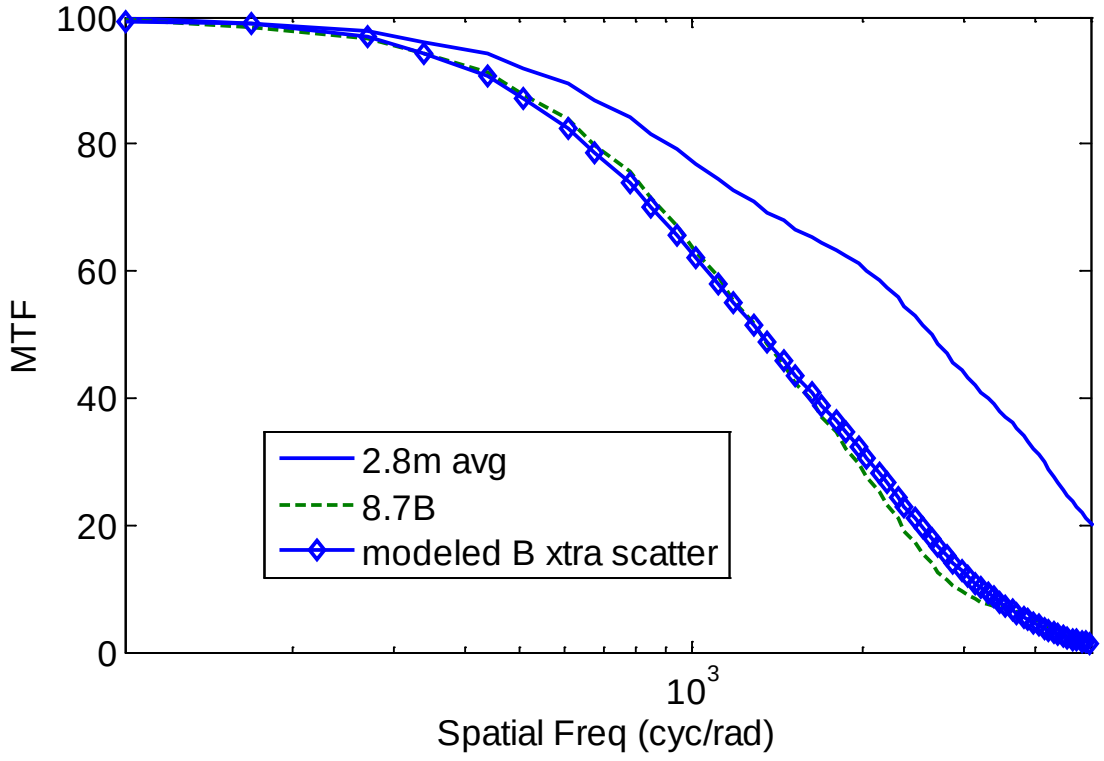
100
80
60
40
20
0
MTF
2.8m avg
8.7B
modeled B xtra scatter
10^3
Spatial Freq (cyc/rad)

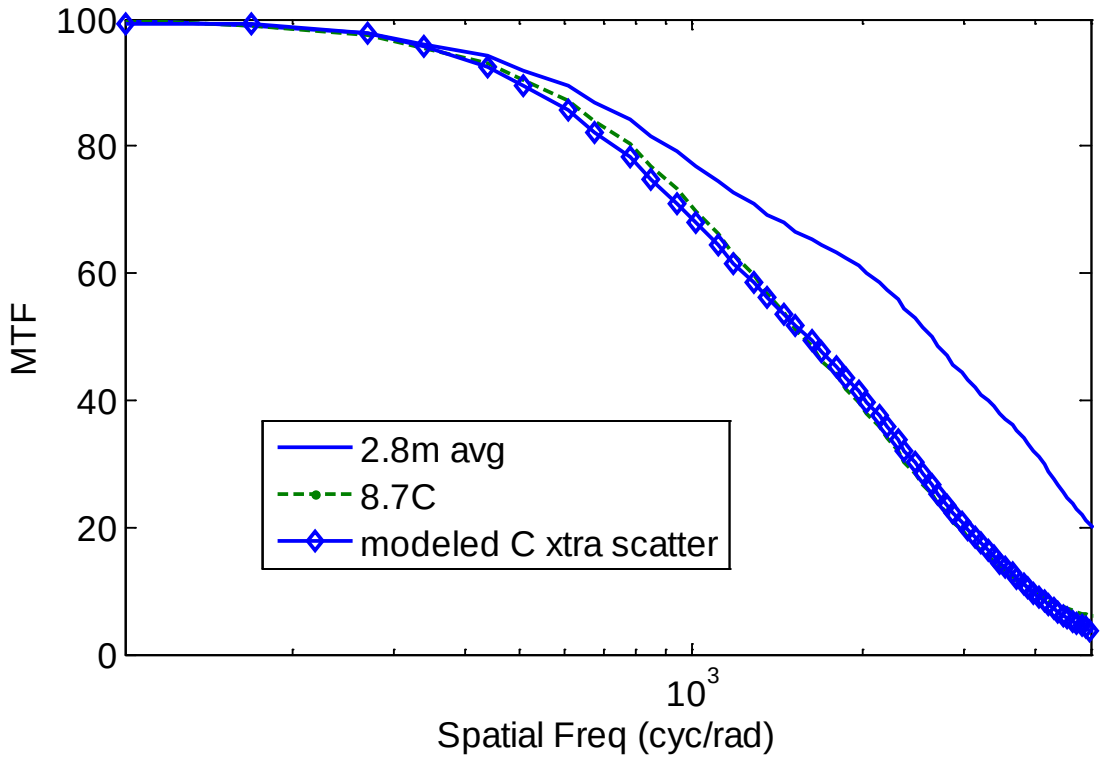

Figure 8. Modulation transfer functions (MTFs) of three different image sequences estimated from 8.7m using the slant edge method, and compared to the modeled results which included extra particle scattering contributions, during July 27 night deployment.